ISSN 0915-633X

NATIONAL INSTITUTE FOR FUSION SCIENCE

Scaling of the Distribution Function and the Critical Exponents near the Point of a Marginal Stability under the Vlasov-Poisson Equations

Alexei Ivanov

(Received - July 3, 2000)

NIFS-639 Aug. 2000

RESEARCH REPORT
NIFS Series

NAGOYA, JAPAN

Scaling of the Distribution Function and the Critical Exponents near the Point of a Marginal Stability under the Vlasov-Poisson Equations

Alexei Ivanov[†]

Theory and Computer Simulation Center, National Institute for Fusion Science, Oroshi-cho, Toki, Gifu, 509-5292, Japan

A model system, described by the consistent Vlassov-Poisson equations under periodical boundary conditions, has been studied numerically near the point of a marginal stability. The power laws, typical for a system, undergoing a second-order phase transition, hold in a vicinity of the critical point: (i) $A \propto -\theta^{\beta}$, $\beta = 1.907 \pm 0.006$ for $\theta \leq 0$, where A is the saturated amplitude of the marginally-stable mode; (ii) $\chi \propto \theta^{-\gamma}$ as $\theta \to 0$, $\gamma = \gamma_{-} = 1.020 \pm 0.008$ for $\theta < 0$, and $\gamma = \gamma_{+} = 0.995 \pm 0.020$ for $\theta > 0$, where $\chi = \partial A / \partial F_1$ at $F_1 \to 0$ is the susceptibility to external drive of the strain F_1; (iii) at $\theta = 0$ the system responds to external drive as $A \propto F_1^{1/\delta}$, and $\delta = 1.544 \pm 0.002$. $\theta = (\langle v^2 \rangle - \langle v_{cr}^2 \rangle)/\langle v_{cr}^2 \rangle$ is the dimensionless reduced velocity dispersion. Within the error of computation these critical exponents satisfy to equality $\gamma = \beta(\delta - 1)$, known in thermodynamics as the Widom equality, which is direct consequence of scaling invariance of the Fourier components f_m of the distribution function f at $|\theta| \ll 1$, i.e. $f_m(\lambda^{a_t} t,\ \lambda^{a_v} v,\ \lambda^{a_\theta}\theta,\ \lambda^{a_{A_0}} A_0,\ \lambda^{a_F} F_1) = \lambda f_m(t, v, \theta, A_0, F_1)$ at $\theta \approx 0$. On the contrary to thermodynamics these critical indices indicate to a very wide critical area. In turn, it means that critical phenomena may determine macroscopic dynamics of a large fraction of systems.

KEY WORDS: Fluctuation phenomena—Phase transitions: general studies—Critical point phenomena

I. INTRODUCTION

First obtained by Ichimaru, Pines, and Rostoker [1], there is the important result, valid for a marginally-stable plasma: a weak stability or a weak instability means that fluctuations with wavenumbers, close to the k_{cr}, can not be stabilized on the level of the particle noise, and may grow large up to the macroscopic level. Even in a stable plasma fluctuations are not a white noise, as it may be intuitively expected, but are concentrated near eigenfunctions [2] because of the long-distance nature of the Coulomb force, and therefore collective behaviour of particles.

The critical state in plasma is similar to the situation, when a medium undergoes a second-order phase transition. In molecular systems phase transitions are accompanied by a wealth of complex phenomena, e.g. critical fluctuations, critical opalescence, etc.

In general, these phenomena are closely related to resonant dynamics. For a trajectory the condition $m\omega_m + l\omega_l = 0$, m and l are integers, implies uncertainty of temporal dynamics. As the insightful study, pioneered by Prof. I. Prigogine [3] and the Brussels-Austin school, shows, the poles of the resolvent of the Liouvillian operator in the spectral domain yield in the collisional term in the Landau or Balescu-Lenard equation [4].

Despite the different physical nature of such systems like gases and ferromagnetic materials, their critical dynamics are quite universal: near the critical point they are described by the power laws for the order parameter, susceptibility, correlation length, specific heat capacity, etc. The critical indices are not arbitrary or independent, but interrelated by equalities like the Widom equality [5]. This universality is a mathematical consequence of deep symmetries of the underlying mathematical structure. Mathematically the Widom equality and other relations for critical indices follow from scaling of the Gibbs potential, which is a homogeneous function near the critical point.

II. MODEL AND THE METHOD

To study the critical dynamics it is more instructive to employ the simplest model, because of complexity of critical phenomena. As a first step, it is useful to consider the case of collisionless gravitating system under periodical boundary conditions. The Jeans gravitational instability [6] is much simpler physically than a plasma instability, so a collisionless system, subjected to this instability at some parameters, is a good model to study these phenomena.

Under these assumptions the governing equations are the Vlassov and the Poisson ones

$$\frac{\partial f}{\partial t} + v\frac{\partial f}{\partial x} - \frac{\partial \Phi}{\partial x}\frac{\partial f}{\partial v} = 0, \tag{1a}$$

$$\frac{\partial^2 \Phi}{\partial x^2} = 4\pi G\left(\int_{-\infty}^{+\infty} f(x, v, t)\, dv - \langle \rho \rangle\right), \tag{1b}$$

$$f(0, v, t) = f(L, v, t), \tag{1c}$$

where f is the distribution function, $\langle \rho \rangle$ is the averaged density, and L is the length of the system. Φ is the gravitational

[†]e-mail alex@nifs.ac.jp

potential, and G is the gravitational constant. Due to periodicity $f(x,v,t)$ can be expanded into the Fourier series as

$$f(x,v,t) = \sum_{m=-\infty}^{\infty} f_m(v,t)\exp(ik_m x), \qquad (2)$$

where $k_m = 2\pi m/L$, m is an integer due to periodic boundary conditions. For $f_m(v,t)$ equations (1a)-(1c) give

$$\dot{f}_m + ik_m v f_m + \\ +i4\pi G \sum_{m=m'+m''} \frac{1}{k_{m'}} \int f_{m'}\, dv \frac{\partial f_{m''}}{\partial v} = 0, \qquad (3)$$

or explicitly for $m = 1, 2$, by truncating at $|m| = 2$

$$\dot{f}_1 + ik_1 v f_1 + i4\pi G \left(\frac{1}{k_1} \int f_1\, dv \cdot \frac{\partial f_0}{\partial v} + \right. \\ + \frac{1}{k_2} \int f_2\, dv \cdot \frac{\partial f_{-1}}{\partial v} + \\ \left. + \frac{1}{k_{-1}} \int f_{-1}\, dv \cdot \frac{\partial f_2}{\partial v} \right) = 0, \qquad (4a)$$

$$\dot{f}_2 + ik_2 v f_2 + i4\pi G \left(\frac{1}{k_2} \int f_2\, dv \cdot \frac{\partial f_0}{\partial v} + \right. \\ \left. + \frac{1}{k_1} \int f_1\, dv \cdot \frac{\partial f_1}{\partial v} \right) = 0. \qquad (4b)$$

The linear stability of this model was studied by Sweet [7] and Lynden-Bell [8]. For the Maxwellian background

$$f_0(v) = \frac{\rho_0}{\sqrt{2\pi}\sigma} \exp\left(-\frac{v^2}{2\sigma^2}\right), \qquad (5)$$

where ρ_0 is the background density, and σ^2 is the velocity dispersion, the dispersion relation is

$$1 - \frac{\sigma_J^2(m)}{\sigma^2} W\left(\frac{\omega_m}{k_m \sigma}\right) = 0, \qquad (6)$$

where $W(Z)$ is the plasma dispersion function, and

$$\sigma_J^2(m) = \frac{4\pi G \rho_0}{k_m^2}, \qquad (7)$$

is the critical velocity dispersion for the mode m.

If $\sigma^2/\sigma_J^2(m) \ll 1$, then $Z \ll 1$, and equation (6) gives for ω_m

$$\omega_m = i\sqrt{\frac{2}{\pi}} k_m \sigma \left[1 - \frac{\sigma^2}{\sigma_J^2(m)}\right]. \qquad (8)$$

Relations (8) shows, that if $\sigma^2 > \sigma_J^2(1)$, then *all* modes are damping, and

$$\lim_{t\to\infty} \rho(x,t) = \rho_0. \qquad (9)$$

After perturbations have damped out, the system becomes invariant against continuous transformation $x' \to x + \alpha$, where α is any number. The situation changes, if $\sigma^2 < \sigma_J^2(1)$. Onset of the instability reduces the initial *continuous* symmetry to the *discrete* transformation $x' \to x + L$. Therefore the value

$$\sigma_{cr}^2 = \frac{4\pi G \rho_0}{k_1^2} \qquad (10)$$

can be assumed as the critical point of the second-order gravitational phase transition after the definition by Landau [9].

A Numerical Algorithm

To integrate equations (1a)-(1c) the method, developed by Cheng and Knorr [10] is used. Evolution is traced by subsequent shifts of the distribution function f in $(x-v)$ plane as follows

$$f^*(x,v) = f^n(x - v\Delta t/2, v) \qquad (11a)$$
$$f^{**}(x,v) = f^*(x, v - a(x)\Delta t) \qquad (11b)$$
$$f^{n+1}(x,v) = f^{**}(x - v\Delta t/2, v). \qquad (11c)$$

Shifting operations are performed using a Fourier interpolation for x-direction and a cubic spline interpolation for v-direction. Computational domain is taken as a rectangular mesh with N mesh point in x-direction, $0 \le x < L$, so the mesh size is $\Delta x = L/N$. In v-direction the domain is divided into the areas of high and low resolution. As it can be seen from further results, the most dynamically important processes occur in the relatively small area of the phase space near $v = 0$. According to equations (3) and (4a)-(4b) the nonlinear evolution is determined by the terms

$$\int f_{m'}\, dv \cdot \frac{\partial f_{m''}}{\partial v},$$

and therefore a sufficient resolution is necessary to reproduce the distribution function. The total number mesh point, M=2000, is taken in v-direction, $|v| \le v_{max}$, where $v_{max} = 4\sigma$ is the cutoff velocity. Equal number of mesh points, $M/2 = 1000$, are adopted for the fine resolution area, $|v| \le v_{fine}$, and for the low resolution area $v_{fine} < |v| \le v_{max}$. So, the mesh sizes in v-direction are

$$\Delta v_{fine} = \frac{2v_{fine}}{M/2 - 1}, \qquad (12a)$$

$$\Delta v_{low} = \frac{2(v_{max} - v_{fine})}{M/2 - 1} \qquad (12b)$$

Timestep is taken from the condition, that two timesteps are required for fastest particles to pass the cell, i.e. $\Delta t = \Delta x/(2v_{max})$.

In x-direction the number of cells might be relatively small, because of only the large scale modes are dynamically important.

In practice $4\pi G = 1$, $\rho_0 = 1$ and $L = 2\pi$ are assumed, so $\sigma_{cr}^2 = 1$, and the characteristic timescale is $t_{dyn} = (\sqrt{G\rho})^{-1} = 2\sqrt{\pi}$.

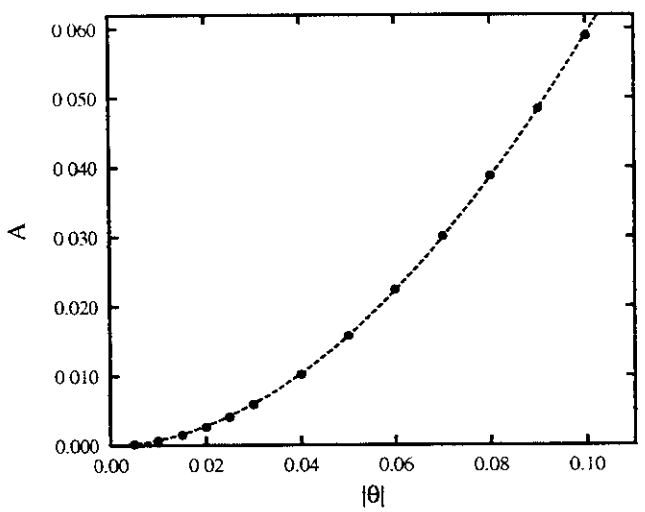

FIG. 1: A as a function of θ. Circles represent experimental data, the dashed line is the power law best fitting approximation.

Depending on the aim, the least number of mesh points in the area of low resolution is 1000, so the lowest value of the recurrence time $t_{rec} = 2\pi/k\Delta v_{low}$ is about $220t_{dyn}$ for $m = 1$ and about $110t_{dyn}$ for $m = 2$.

III. ORDER PARAMETER

For calculation of the critical indices the order parameter must be first defined as a quantity, which is nonzero below the critical point, and is equal to zero above it [9]. Expansion of the density $\rho = \rho(t, x; \sigma_0^2)$ into the Fourier series gives

$$\rho(t, x; \sigma_0^2) = \sum_{m=-\infty}^{\infty} \rho_m(t, \sigma_0^2) \exp(ik_m x), \qquad (13)$$

where σ_0^2 is the velocity dispersion at the starting moment $t = 0$. Instead of σ_0^2 it is more convenient to use the dimensionless velocity dispersion θ, defined as

$$\theta = \frac{\sigma_0^2 - \sigma_{cr}^2}{\sigma_{cr}^2}. \qquad (14)$$

Let

$$\tilde{A}_m(t, \theta) = |\rho_m(t, \theta)|. \qquad (15)$$

According to dispersion relation (8) and limit (9)

$$\tilde{A}_1(t, \theta) = \begin{cases} \tilde{A}_1 > 0, & \text{if } \theta \leq 0; \\ 0, & \text{if } \theta > 0 \end{cases} \qquad (16)$$

In absence of collisions there are no equilibrium values of $\tilde{A}_m$ when

$$\frac{\partial \tilde{A}_m}{\partial t} = 0 \qquad (17)$$

is valid. However, the use of the saturated amplitudes of $\tilde{A}_m$, computed in a run, i.e.

$$A_m(\theta) = \max\{\tilde{A}_m(t, \theta), 0 \leq t \leq t_{end}\}, \qquad (18)$$

gives time-independent quantities and allows to study only the θ-dependence. The similar quantity was used by Lee et al. [11] and Watanabe, Sugama, and Sato [12] to describe the dependence of the saturated amplitude of the electric field on the imaginary part of the eigenfrequency for the ion temperature gradient drift instability in collisionless plasma.

So, the order parameter is finally defined as

$$A(\theta) \equiv A_1(\theta). \qquad (19)$$

IV. CRITICAL EXPONENTS

A Order Parameter and the Index β

To calculate the saturated amplitude $A(\theta)$, the initial perturbation in the form $\tilde{\rho}(x) = A_0 \cos(k_m x)$, where $m = 1$, and the amplitude of the perturbation $A_0 = 10^{-5}$ is imposed on the system, and then equations (1a)-(1c) have been integrated until the saturated amplitude has reached. As Fig. 1 shows, A is a well defined function of θ. A best-fitting approximation confirms with a good accuracy that A depends on θ as a power law, i.e.

$$A \propto -\theta^{\beta}, \quad \theta \leq 0, \qquad (20)$$

and

$$\beta = 1.907 \pm 0.006.$$

Since stabilization is due to the nonlinear terms of equation (1a) (or equation (3), and (4a-4b)), the resolution of the mesh must be detailed enough to reproduce correctly the structure of the f_m components of the distribution function in the velocity space. To illustrate this, calculations have been performed on equidistant mesh with the mesh size in v-direction

$$\Delta v = \frac{2v_{max}}{M - 1}, \qquad (21)$$

and $M = \{50, 100, 200, 500, 2000\}$. The calculated indices β for these M are listed in Table I.

Fig. 2, where the real and imaginary parts of f_m components, $m = 1, 2, 3$, for the cases $M = 100$ and $M = 2000$ are

TABLE I: β vs. resolution in the velocity domain.

N	M	β
16	50	1.084 ± 0.046
16	100	1.564 ± 0.022
16	200	1.856 ± 0.008
16	500	1.873 ± 0.004
16	2000	1.872 ± 0.004

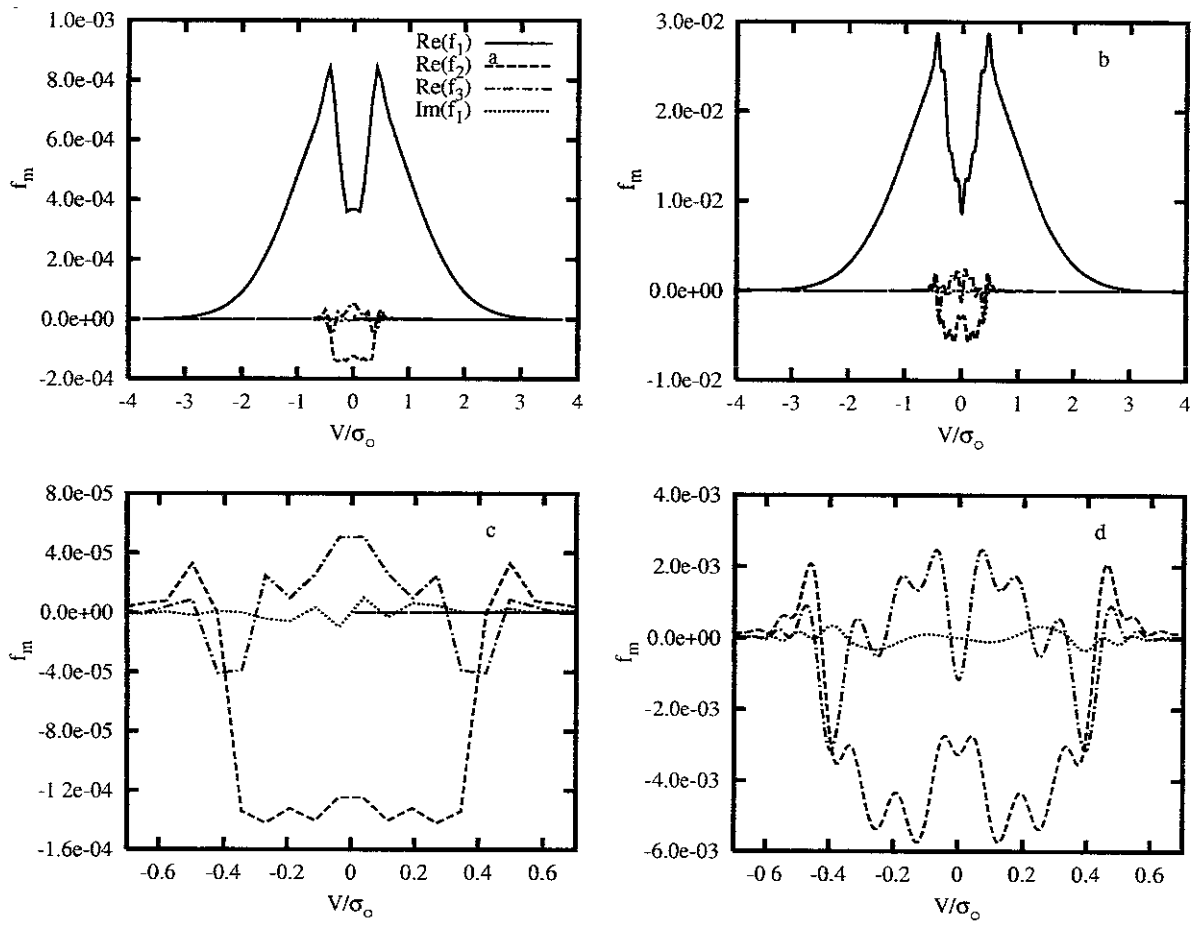

FIG. 2: Distribution in the velocity space for real and imaginary parts of the Fourier components of $f(x, v, t)$ for $\theta = -0.1$ and for the time moment when $\tilde{A}_1(t, \theta) = A$. Solid line corresponds to the $Re[f_1(v)]$, long-dashed line corresponds to $Re[f_2(v)]$, dashed line, close to $x = 0$, corresponds to $Im[f_1(v)]$. For the left plot $M = 100$, (a), (c), for the right $M = 2000$, (b), (d).

plotted, is more illustrative. Insufficient resolution and recurrence wipes out the fine structure in the velocity domain and influences significantly on calculation of the critical exponent β.

Value $\beta \approx 1.907 > 1$ is untypical for this index and indicates to significant differences between the critical dynamics of thermodynamic systems and gravitating ones. For comparison, for such gases as Ar, Xe, CO_2, Helium-4 experimental value $\beta \approx 0.35 < 1$. It means, that

$$\lim_{\theta \to -0} \frac{\partial n}{\partial \theta} = -\infty, \tag{22}$$

where n is the order parameter for these transitions, while for the gravitating system, studied here, the following is valid

$$\lim_{\theta \to -0} \frac{\partial A}{\partial \theta} = 0. \tag{23}$$

However, $\beta \geq 1$ seems not to be unusual for collisionless systems under kinetic description. As equation (43) in Lee et al. [11] and Watanabe, Sugama, and Sato [12] results show, for the ion temperature gradient drift instability there also exists the scaling as $\beta = 1$ between the peak (saturated) value of the first (the least k) harmonic of the electric field and the imaginary part of the eigenfrequency. What is more interesting, these authors considered as negligible the nonlinearity

$$\int f_{m'}\, dv \cdot \frac{\partial f_{m''}}{\partial v},$$

so in some sense their assumptions lead to a similar situation, as in the case of insufficient resolution at $M = 50$.

This result indicates, that symmetry change in a gravitating system can be a very mild process, unlike thermodynamics and its flashing emergence of a new phase, but it also means that gravitational phase transitions, unlike their thermodynamic counterparts, *are not necessarily fine tuned phenomena* and the critical area can be very wide.

Another interesting result is a relatively small amplitude of the peak value of the order parameter. Even if the system is assumed relatively far from stability, it is about 6 percent at $\theta = -0.1$. It also means that stochastic and deterministic processes may compete in a wide area $\Delta\theta$ at $\theta = 0$.

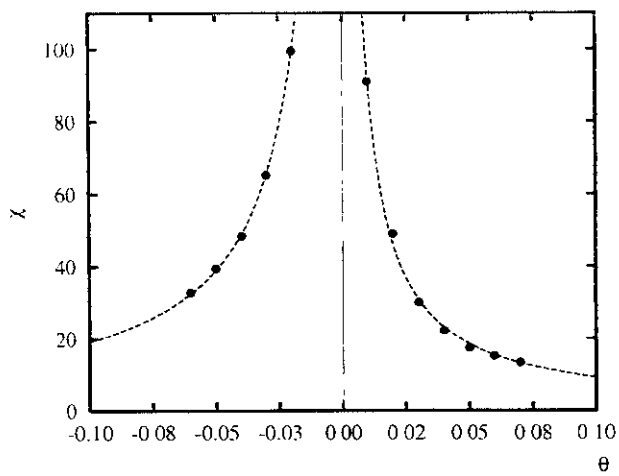

FIG. 3. χ as a function of θ. Circles represent experimental data, the dashed lines are the power law best fit approximations.

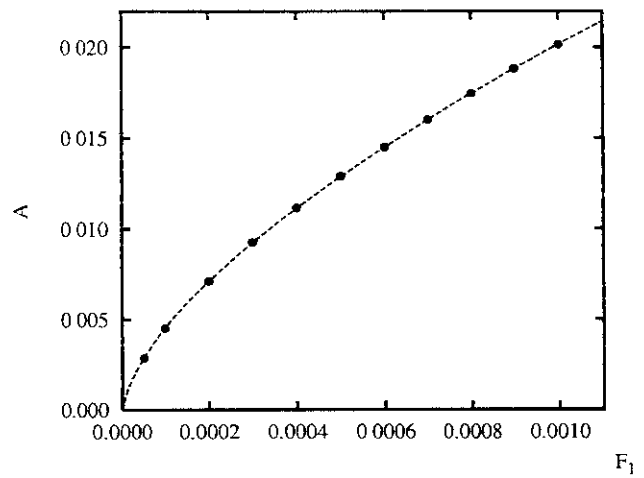

FIG. 4: A as a function of F_1. Circles represent experimental data, the dashed lines are the power law best fit approximations.

B Susceptibility at $\theta \lesssim 0$, and the Response at $\theta = 0$: Critical Indexes γ and δ

The susceptibility to the external drive in the form

$$F(x) = F_m \cos(k_m x + \varphi) \tag{24}$$

can be determined as the ratio of response $A_m(\theta)$ to the strain F_m of the drive, i.e.

$$\chi_m(\theta) = \left.\frac{\partial A_m(\theta)}{\partial F_m}\right|_{F_m \to 0}. \tag{25}$$

The main difficulty of calculations of $\chi(\theta) \equiv \chi_1(\theta)$ at $\theta \approx 0$ is the necessity to take F_1 very small to provide the linear dependence A on θ at $\theta \simeq 10^{-2}$. Therefore F_1 is assumed very small, $F_1 < 10^{-6}$, and a long time is required until the saturated amplitude A has reached.

The results are plotted in Fig. 3 for $\theta < 0$ and $\theta > 0$. As it can be seen from the plot, the shape of the susceptibility is a typical λ-curve, usual for the response functions like the specific heat or compressibility at the critical point (Stanley [13] and references therein).

The best fitting approximation gives for $\chi(\theta)$

$$\chi \propto \theta^{-\gamma_\pm}, \tag{26}$$

and

$$\gamma_- = 1.020 \pm 0.008, \quad \theta < 0, \tag{27a}$$

$$\gamma_+ = 0.995 \pm 0.020, \quad \theta > 0. \tag{27b}$$

The response A in the critical point $\theta = 0$ is described by the exponent δ. The results are plotted in Fig. 4, and the function $A = A(F_1)$ at $\theta = 0$ can be approximated as

$$A \propto F_1^{1/\delta}, \tag{28}$$

and

$$\delta = 1.544 \pm 0.002.$$

V. SCALING OF THE DISTRIBUTION FUNCTION AND THE WIDOM EQUALITY

In thermodynamics there is the interrelation between the exponents β, γ, and δ, known as the Widom equality [5]

$$\gamma = \beta(\delta - 1), \tag{29}$$

which follows from the scaling invariance of the Gibbs potential near the critical temperature T_{cr} as

$$G(\lambda^{a_\epsilon}\epsilon, \lambda^{a_M} M) = \lambda G(\epsilon, M), \tag{30}$$

where M is magnetization, and $\epsilon = (T - T_{cr})/T_{cr} \approx 0$ is the dimensionless temperature. When substituted to (29) the exponents β, γ, and δ, calculated for collisionless gravitation, satisfy to it with a good accuracy, suggesting existence of the symmetries, like the symmetry of the Gibbs potential with respect to scaling transformations.

However for the case, studied here, the functions are time dependent. The solution is to take snapshots of the dynamics at some characteristic moment, e.g. at the saturation time $t = t_{sat}$, when $\tilde{A}_1(t.\theta)$ reaches its saturated value A, i.e. $\tilde{A}_1(t_{sat}, \theta) = A$. The results are shown in Fig. 5 for three types of conditions: 1) $\theta = -0.01$, $A_0 = 10^{-5}$; 2) $\theta = -0.04$, $A_0 = 10^{-5}$; 3) $\theta = -0.04$, $A_0 = 10^{-4}$. The upper and the second row corresponds to the time moments when $\tilde{A}_1(t, \theta)$ hits its first maximum, A, the third row - to the moment when $\tilde{A}_1(t, \theta)$ hits its second maximum. These moments *are different* for these three types of conditions: for the first case the moments of the first and the second maxima are $183.14\, t_{dyn}$ and $386.96\, t_{dyn}$; for the second case - $69.65\, t_{dyn}$ and $119.74\, t_{dyn}$; for the third - $49.24\, t_{dyn}$ and $99.27\, t_{dyn}$.

But with exception of minor differences because of discreteness of calculations *the structure of the distribution function is the same for all of these conditions.*

The same is valid for calculations of the critical indices δ and γ for $\theta = 0$ as well as for $\theta \lesssim 0$ at $F_1 \neq 0$: when

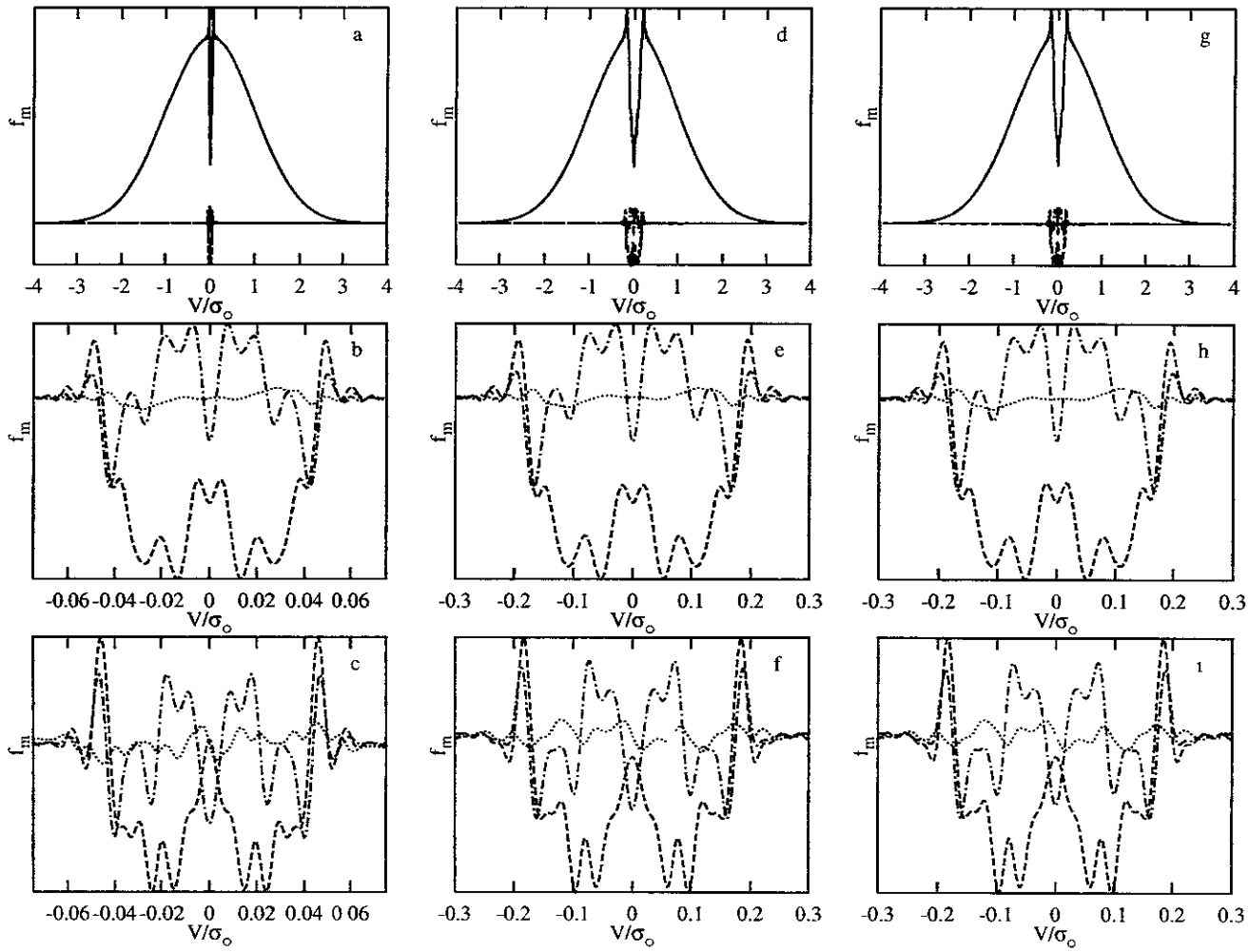

FIG. 5: Scaling of the Fourier components f_m for three types of initial conditions: (a)-(c) $\theta = -0.01$, $A_0 = 10^{-5}$; (d)-(f) $\theta = -0.04$, $A_0 = 10^{-5}$; (g)-(i) $\theta = -0.04$, $A_0 = 10^{-4}$. The notation for lines are the same as for Fig. 2. The upper and the middle rows correspond to the time moment $t = t_{sat}$, the bottom row corresponds to the time moment, when $\tilde{A}_1(t,\theta)$ hits its second maximum.

$A = A(t,\theta,F_1)$ hits its first and second maxima, the structure of the f_m is the same for different θ and strains F_1, and, correspondingly, times.

It allows to conclude, that *near the critical point* $\theta = 0$ *the Fourier component* f_m *of the distribution functions is a homogeneous function of its arguments*, i.e.

$$f_m(\lambda^{a_t}t,\ \lambda^{a_v}v,\ \lambda^{a_\theta}\theta,\ \lambda^{a_{A_0}}A_0,\ \lambda^{a_F}F_1) = \\ = \lambda f_m(t,v,\theta,A_0,F_1), \quad (31)$$

and so is the entire distribution function, i.e.

$$f(\lambda^{a_t}t,\ \lambda^{a_v}v,\ \lambda^{a_\theta}\theta,\ \lambda^{a_{A_0}}A_0,\ \lambda^{a_F}F_1) = \\ = \lambda f(t,v,\theta,A_0,F_1). \quad (32)$$

The last equality makes proof of equality (29) straightforward, which is done in Appendix for the case, considered in this paper.

A Critical Exponents for the Saturation Times t_{sat}

As it follows from homogeneity assumptions (31)-(32) and its corollary (A2), the saturation times, t_{sat}, are not arbitrary values, but are some functions of θ, A_0, F_1, i.e.

$$t_{sat} = t_{sat}(\theta,A_0,F_1). \quad (33)$$

The saturation time t_{sat} is shown in Fig. 6a as a function of the strain F_1 of the external drive at $\theta = 0$, $A_0 = 0$, and in Fig. 6b as a function of θ at $A_0 = 10^{-5}$, $F_1 = 0$. In the both cases t_{sat} can be approximated by power laws, i.e.

$$t_{sat} \propto F_1^{-\Delta}, \quad \Delta = 0.3423 \pm 0.0004, \quad (34)$$

and

$$t_{sat} \propto (-\theta)^{-B}, \quad B = 0.647 \pm 0.015. \quad (35)$$

Saturation times diverges as $\theta \to 0$, $F_1 \to 0$.

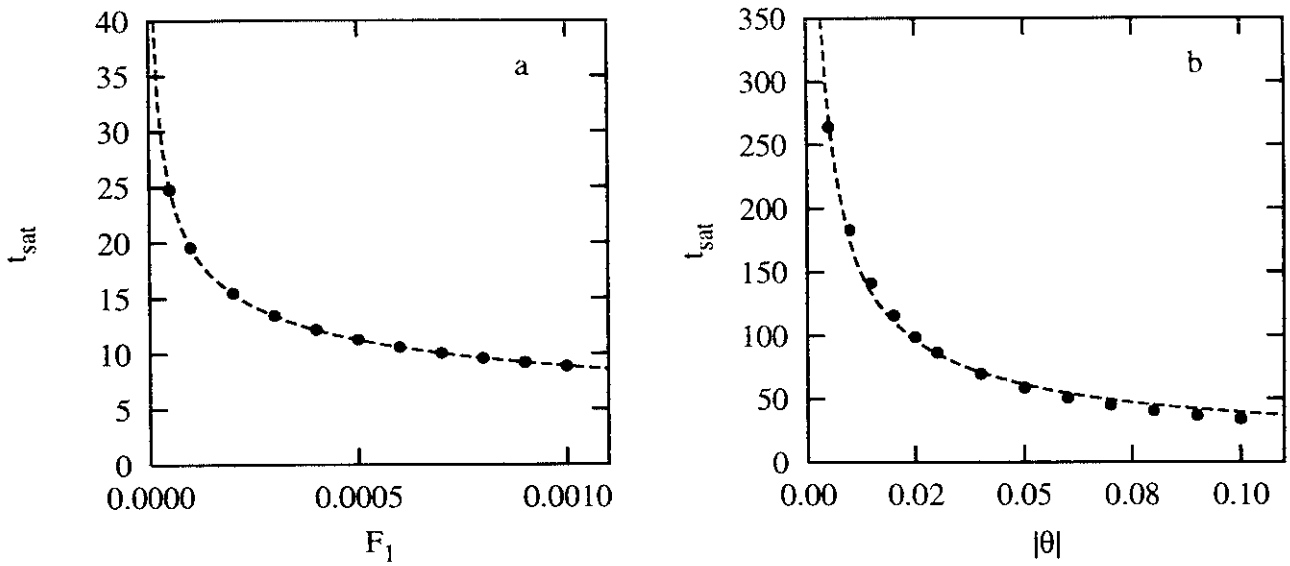

FIG. 6: Saturation time t_{sat}: (a) as a function of the strain F_1 of the external driving at $\theta = 0$, $A_0 = 0$; (b) as a function of $|\theta|$, $\theta < 0$ at $A_0 = 10^{-5}$, $F_1 = 0$.

While instructive, relations (34) and (35) are not universal: in general, t_{sat}, given by equation (33), is a hypersurface, and relations (34) and (35) can be treated as its sections. At $F_1 = 0$, $\theta < 0$ this section is a two-dimensional surface, plotted in Fig. 7.

VI. THE WIDTH OF THE CRITICAL AREA

As χ diverges for $m = 1$ as $\theta \to 0$, χ_m remains finite at $\theta = 0$ for $m \neq 1$. It indicates that at $\theta \approx 0$ the incoherent particle noise may grow into a coherent structure of $k \approx k_1$ of the level up to the macroscopic level amplitude. This stochastic excitation of a coherent structure was observed in hydrodynamic simulations of the model under periodical boundary conditions if the density and the velocity were assumed disturbing randomly on each timestep by the Langevin sources, incorporating thermodynamic noises [14]. Near the critical state fluctuations of small amplitude grow to a highly coherent spatial structure of the Jeans wavelength, but of a random amplitude and phase. For this model the critical index $\beta = 1/2$ has been calculated, the others are, of course, of the classical Landau-Weiss set: $\gamma = 1$, and $\delta = 3$.

Such excitation occurs in the collisionless self-gravitating model followed by the N-body simulation [15]. Besides of the values of the critical indices the process is similar to hydrodynamics, but, while distinct, this selective growth of fluctuations at $k \approx k_{cr}$ is not so sharp as in the hydrodynamic simulations.

For thermodynamics the typical value is $\delta \approx 4$. One can estimate the relative level of critical fluctuations using the power law (28). If the total mass of the system is M_{tot}, and the number of particles is N_p then the instant density is

$$\rho = \frac{1}{V}\frac{M_{tot}}{N_p}N_p = \frac{1}{V}\frac{\langle M\rangle + \delta M}{\langle N\rangle + \delta N}(\langle N\rangle + \delta N) \approx$$
$$\approx \langle\rho\rangle + \langle\rho\rangle\frac{2\,\delta N}{\langle N\rangle} \sim \langle\rho\rangle + \frac{\langle\rho\rangle}{\sqrt{N_p}},$$

and thermodynamic fluctuations of density $\delta\rho$ are

$$\delta\rho \sim \langle\rho\rangle\frac{1}{\sqrt{N_p}}. \tag{36}$$

Since

$$\delta F_1 = i4\pi G\frac{\delta\rho_1}{k_1}, \tag{37}$$

where $\delta\rho_1$ and δF_1 are, respectively, the Fourier components of fluctuations of the density and acceleration for $m = 1$. Therefore

$$\delta A \sim N_p^{-1/(2\delta)} \quad \text{at} \quad \theta = 0. \tag{38}$$

If $N_p = N_A \approx 6 \cdot 10^{23}$, then thermodynamic fluctuations are $\sim 10^5$ larger than the gravitational ones.

Equation (38) together with equation (20) gives the estimation of the width of the critical area $\Delta\theta$, where chaotic dynamics are of the same importance as deterministic ones, i.e.

$$A \approx \delta A, \tag{39}$$

so

$$\Delta\theta \sim N_p^{-1/(2\beta\delta)}. \tag{40}$$

For $N = N_A$ and for the case of thermodynamics with $\delta \approx 4$ and $\beta \approx 0.3$

$$\Delta\theta_{th} \sim 10^{-9}.$$

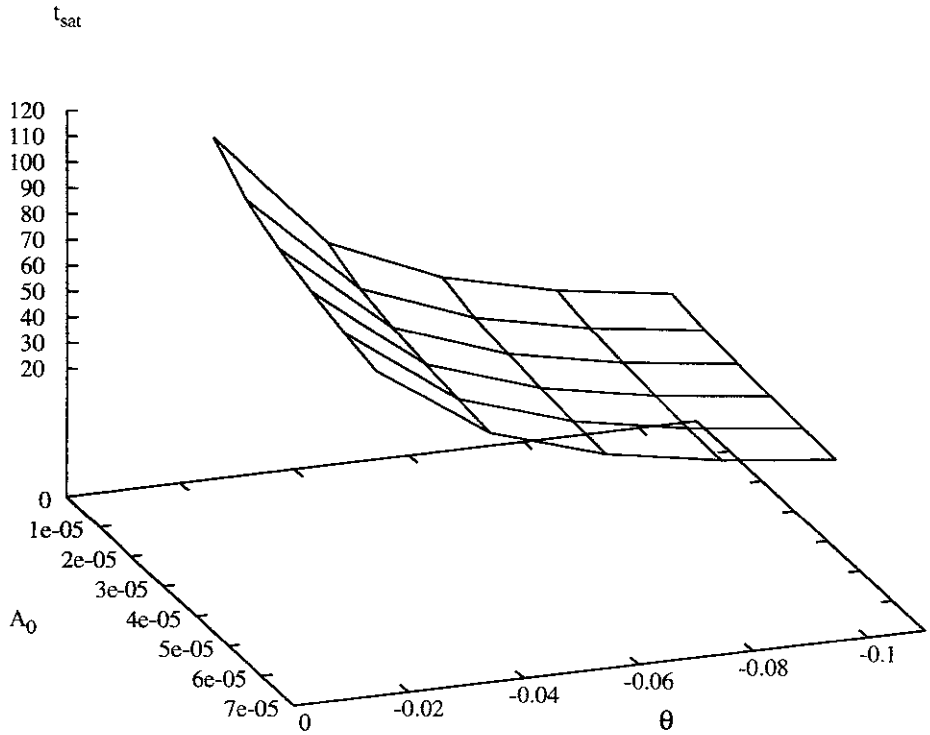

FIG. 7: Saturation time t_{sat} as a function of θ and A_0, $t_{sat} = t_{sat}(\theta, A_0)$, $F_1 = 0$.

In the case of gravitation with $\delta \approx 1.54$, $\beta \approx 1.91$

$$\Delta\theta_{gr} \sim 10^{-4},$$

which is in 10^5 times greater then for thermodynamics.

ACKNOWLEDGMENTS

I express my deep gratitude to Prof. T. Sato and to Prof. K. Watanabe for valuable discussions. I wish to acknowledge valuable conversation with Dr. A. Kageyama and Dr. T.-H. Watanabe. I highly appreciate valuable comments of Prof. Vadim Antonov and Prof. Leonid Ossipkov. This paper was written during the Post-Doctoral Fellowship term in the National Institute for Fusion Science, Japan under financial support of the Japan Society for the Promotion of Science in the FY 1999, for which I am particularly indebted.

APPENDIX A: PROOF OF THE WIDOM EQUALITY FOR THE GRAVITATIONAL DYNAMICS

Let for simplicity change the sign of the power index at v variable, i.e. the homogeneity condition (31) for f_m is rewritten as

$$f_m(\lambda^{a_t} t,\ \lambda^{-a_v} v,\ \lambda^{a_\theta}\theta,\ \lambda^{a_{A_0}} A_0,\ \lambda^{a_F} F_1) = \\ = \lambda f_m(t, v, \theta, A_0, F_1), \quad \text{(A1)}$$

Integration of (A1) on v variable gives for $\tilde{A}_m$ components

$$\lambda^{a_v}\tilde{A}_m(\lambda^{a_t} t,\ \lambda^{a_\theta}\theta,\ \lambda^{a_{A_0}} A_0,\ \lambda^{a_F} F_1) = \\ = \lambda\tilde{A}_m(t, \theta, A_0, F_1). \quad \text{(A2)}$$

Because of $\tilde{A}_m$ is considered at the moment $t = t_{sat}$ it allows to exclude its time dependence and to write for $A \equiv A_1$

$$\lambda^{a_v} A(\lambda^{a_\theta}\theta,\ \lambda^{a_{A_0}} A_0,\ \lambda^{a_F} F_1) = \lambda A(\theta, A_0, F_1). \quad \text{(A3)}$$

If the initial perturbation $A_0 \equiv |\rho_1(t, \theta)|$ at $t = 0$ is taken such as $|\rho_1(0, \theta)| \ll \rho_0$, then, as calculations show A_m is almost independent on A_0, and therefore one can write

$$\lambda^{a_v} A(\lambda^{a_\theta}\theta,\ \lambda^{a_F} F_1) = \lambda A(\theta, F_1). \quad \text{(A4)}$$

Equation (A4) is the same as equation (11.32) in Stanley [13] and the following treatment is straightforward. For the case $\theta \to 0$ and $F_1 = 0$ equation (A4) becomes

$$A(\theta, 0) = \lambda^{a_v - 1} A(\lambda^{a_\theta}\theta, 0). \quad \text{(A5)}$$

Without loss of the generality one can choose $\lambda = (-1/\theta)^{1/\theta}$ so

$$A(\theta, 0) = -\theta^{(1-a_v)/a_\theta} A(-1, 0). \quad \text{(A6)}$$

But from equation (20) $A(\theta, 0) \sim (-\theta)^\beta$, and therefore

$$\beta = \frac{1 - a_v}{a_\theta}. \quad \text{(A7)}$$

If to set $\theta = 0$, $F_1 \to 0$, then

$$A(0, F_1) = \lambda^{a_v - 1} A(0, \lambda^{a_F} F_1), \quad \text{(A8)}$$

and by the same way, with $\lambda = F_1^{-1/a_F}$ equation (A8) becomes

$$A(0, F_1) = F_1^{(1-a_v)/a_F} A(0, 1). \quad \text{(A9)}$$

But according to equation (28) $A \sim F_1^{1/\delta}$ whence

$$\delta = \frac{a_F}{1 - a_v}. \quad \text{(A10)}$$

On differentiating (A4) with respect to F_1 one can obtain

$$\lambda^{a_v + a_F} \chi(\lambda^{a_\theta} \theta, \lambda^{a_F} F_1) = \lambda \chi(\theta, F_1). \quad \text{(A11)}$$

For the particular choice $\lambda = (-\theta)^{-1/a_\theta}$ and $F_1 = 0$

$$\chi(\theta, 0) = \theta^{-(a_v + a_F - 1)/a_\theta} \chi(-1, 0), \quad \text{(A12)}$$

and according to the equation (26) $\chi(\theta, 0) = \theta^{-\gamma_-}$ at $\theta \to -0$ whence

$$\gamma_- = \frac{a_v + a_F - 1}{a_\theta}. \quad \text{(A13)}$$

If to consider $\lambda = (\theta)^{-1/a_\theta}$ one can write for γ_+ in the same way

$$\gamma_+ = \frac{a_v + a_F - 1}{a_\theta}, \quad \text{(A14)}$$

and therefore

$$\gamma_- = \gamma_+ = \gamma = \frac{a_v + a_F - 1}{a_\theta} = \\ = \frac{a_v - 1}{a_\theta} + \frac{a_F}{a_\theta} = -\beta + \delta\beta, \quad \text{(A15)}$$

and finally

$$\gamma = \beta(\delta - 1). \quad \text{(A16)}$$

REFERENCES

[1] S. Ichimaru S, D. Pines, and N. Rostoker, Phys. Rev. Lett. **8**, 231 (1962).

[2] A.F. Alexandrov, L.S. Bogdankevich, and A.A Rukhadze, *Principles of plasma electrodynamics* (Berlin: Springer-Verlag, 1984).

[3] I. Prigogine, *Non-Equilibrium Statistical Mechanics* (New York: Interscience Publishers, 1962).

[4] R. Balescu, *Statistical mechanics of charged particles* (London: Interscience Publishers, 1963).

[5] B. Widom, J. Chem. Phys, **41**, 1633 (1964).

[6] J. Jeans *Astronomy and cosmogony* (The University Press: Cambridge, 1928).

[7] P.A. Sweet, Mon. Not. R. astron. Soc., **125**, 285 (1963).

[8] D. Lynden-Bell, in *Relativity Theory and Astrophysics, vol.2, Galactic Structure*, edited by J. Ehlers (Providence, RI: Am. Math. Soc. 1967), p. 131.

[9] L.D. Landau and E.M. Lifshitz, *Statistical physics* (Oxford: Pergamon, 1980).

[10] C.Z. Cheng, and G. Knorr, J. Comput. Phys. **22**, 330 (1976).

[11] W.W. Lee, J.A. Krommes, K.R. Oberman, and R.A. Smith, Phys. Fluids, **27**, 2652 (1984).

[12] T.-H. Watanabe, H. Sugama, and T. Sato, Physics of Plasmas, **7**, 984 (2000).

[13] H.E. Stanley, *Introduction to Phase Transitions and Critical Phenomena* (Oxford: Clarendon Press. 1971).

[14] A.V. Ivanov, Astroph. and Sp. Sci., **159**, 47 (1989).

[15] A.V. Ivanov, Mon. Not. R. astron. Soc., **259**, 576 (1992).

Recent Issues of NIFS Series

NIFS-576 S. Murakami, U. Gasparino, H. Idei, S. Kubo, H. Maassberg, N. Marushchenko, N. Nakajima, M. Romé and M. Okamoto,
5D Simulation Study of Suprathermal Electron Transport in Non-Axisymmetric Plasmas, Oct. 1998
(IAEA-CN-69/THP1/01)

NIFS-577 S. Fujiwara and T. Sato,
Molecular Dynamics Simulation of Structure Formation of Short Chain Molecules; Nov. 1998

NIFS-578 T. Yamagishi,
Eigenfunctions for Vlasov Equation in Multi-species Plasmas Nov. 1998

NIFS-579 M. Tanaka, A. Yu. Grosberg and T. Tanaka,
Molecular Dynamics of Strongly-Coupled Multichain Coulomb Polymers in Pure and Salt Aqueous Solutions; Nov. 1998

NIFS-580 J. Chen, N. Nakajima and M. Okamoto,
Global Mode Analysis of Ideal MHD Modes in a Heliotron/Torsatron System: I. Mercier-unstable Equilibria; Dec. 1998

NIFS-581 M. Tanaka, A. Yu. Grosberg and T. Tanaka,
Comparison of Multichain Coulomb Polymers in Isolated and Periodic Systems: Molecular Dynamics Study; Jan. 1999

NIFS-582 V.S. Chan and S. Murakami,
Self-Consistent Electric Field Effect on Electron Transport of ECH Plasmas; Feb. 1999

NIFS-583 M. Yokoyama, N. Nakajima, M. Okamoto, Y. Nakamura and M. Wakatani,
Roles of Bumpy Field on Collisionless Particle Confinement in Helical-Axis Heliotrons; Feb. 1999

NIFS-584 T.-H. Watanabe, T. Hayashi, T. Sato, M. Yamada and H. Ji,
Modeling of Magnetic Island Formation in Magnetic Reconnection Experiment; Feb. 1999

NIFS-585 R. Kumazawa, T. Mutoh, T. Seki, F. Shinpo, G. Nomura, T. Ido, T. Watari, Jean-Marie Noterdaeme and Yangping Zhao,
Liquid Stub Tuner for Ion Cyclotron Heating; Mar. 1999

NIFS-586 A. Sagara, M. Iima, S. Inagaki, N. Inoue, H. Suzuki, K. Tsuzuki, S. Masuzaki, J. Miyazawa, S. Morita, Y. Nakamura, N. Noda, B. Peterson, S. Sakakibara, T. Shimozuma, H. Yamada, K. Akaishi, H. Chikaraishi, H. Funaba, O. Kaneko, K. Kawahata, A. Komori, N. Ohyabu, O. Motojima, LHD Exp. Group 1, LHD Exp. Group 2,
Wall Conditioning at the Starting Phase of LHD, Mar. 1999

NIFS-587 T. Nakamura and T. Yabe,
Cubic Interpolated Propagation Scheme for Solving the Hyper-Dimensional Vlasov-Poisson Equation in Phase Space; Mar. 1999

NIFS-588 W.X. Wnag, N. Nakajima, S. Murakami and M. Okamoto,
An Accurate δf Method for Neoclassical Transport Calculation, Mar. 1999

NIFS-589 K. Kishida, K. Araki, S. Kishiba and K. Suzuki,
Local or Nonlocal? Orthonormal Divergence-free Wavelet Analysis of Nonlinear Interactions in Turbulence; Mar. 1999

NIFS-590 K. Araki, K. Suzuki, K. Kishida and S. Kishiba,
Multiresolution Approximation of the Vector Fields on T^3; Mar. 1999

NIFS-591 K. Yamazaki, H. Yamada, K.Y. Watanabe, K. Nishimura, S. Yamaguchi, H. Nakanishi, A. Komori, H. Suzuki, T. Mito, H. Chikaraishi, K. Murai, O. Motojima and the LHD Group,

Overview of the Large Helical Device (LHD) Control System and Its First Operation; Apr. 1999

NIFS-592 T. Takahashi and Y. Nakao,
Thermonuclear Reactivity of D-T Fusion Plasma with Spin-Polarized Fuel; Apr. 1999

NIFS-593 H. Sugama,
Damping of Toroidal Ion Temperature Gradient Modes; Apr. 1999

NIFS-594 Xiaodong Li,
Analysis of Crowbar Action of High Voltage DC Power Supply in the LHD ICRF System; Apr. 1999

NIFS-595 K. Nishimura, R. Horiuchi and T. Sato,
Drift-kink Instability Induced by Beam Ions in Field-reversed Configurations; Apr. 1999

NIFS-596 Y. Suzuki, T-H. Watanabe, T. Sato and T. Hayashi,
Three-dimensional Simulation Study of Compact Toroid Plasmoid Injection into Magnetized Plasmas; Apr. 1999

NIFS-597 H. Sanuki, K. Itoh, M. Yokoyama, A. Fujisawa, K. Ida, S. Toda, S.-I. Itoh, M. Yagi and A. Fukuyama,
Possibility of Internal Transport Barrier Formation and Electric Field Bifurcation in LHD Plasma,
May 1999

NIFS-598 S. Nakazawa, N. Nakajima, M. Okamoto and N. Ohyabu,
One Dimensional Simulation on Stability of Detached Plasma in a Tokamak Divertor; June 1999

NIFS-599 S. Murakami, N. Nakajima, M. Okamoto and J. Nhrenberg,
Effect of Energetic Ion Loss on ICRF Heating Efficiency and Energy Confinement Time in Heliotrons;
June 1999

NIFS-600 R. Horiuchi and T. Sato,
Three-Dimensional Particle Simulation of Plasma Instabilities and Collisionless Reconnection in a Current Sheet;; June 1999

NIFS-601 W. Wang, M. Okamoto, N. Nakajima and S. Murakami,
Collisional Transport in a Plasma with Steep Gradients; June 1999

NIFS-602 T. Mutoh, R. Kumazawa, T. Saki, K. Saito, F. Simpo, G. Nomura, T. Watari, X. Jikang, G. Cattanei, H. Okada, K. Ohkubo, M. Sato, S. Kubo, T Shimozuma, H. Idei, Y. Yoshimura, O. Kaneko, Y Takeiri, M. Osakabe, Y Oka, K Tsumori, A. Komori, H. Yamada, K. Watanabe, S. Sakakibara, M. Shoji, R. Sakamoto, S. Inagaki, J. Miyazawa, S. Morita, K. Tanaka, B.J. Peterson, S. Murakami, T. Minami, S. Ohdachi, S. Kado, K. Narihara, H. Sasao, H. Suzuki, K. Kawahata, N. Ohyabu, Y Nakamura, H. Funaba, S. Masuzaki, S. Muto, K. Sato, T. Morisaki, S. Sudo, Y Nagayama, T. Watanabe, M. Sasao, K. Ida, N. Noda, K. Yamazaki, K. Akaishi, A. Sagara, K Nishimura, T. Ozaki, K Toi, O Motojima, M. Fujiwara, A. Iiyoshi and LHD Exp Group 1 and 2,
First ICRF Heating Experiment in the Large Helical Device; July 1999

NIFS-603 P.C. de Vries, Y. Nagayama, K. Kawahata, S. Inagaki, H. Sasao and K. Nagasaki,
Polarization of Electron Cyclotron Emission Spectra in LHD; July 1999

NIFS-604 W. Wang, N. Nakajima, M. Okamoto and S. Murakami,
δf Simulation of Ion Neoclassical Transport; July 1999

NIFS-605 T. Hayashi, N. Mizuguchi, T Sato and the Complexity Simulation Group,
Numerical Simulation of Internal Reconnection Event in Spherical Tokamak; July 1999

NIFS-606 M. Okamoto, N. Nakajima and W. Wang,
On the Two Weighting Scheme for δf Collisional Transport Simulation; Aug. 1999

NIFS-607 O Motojima, A.A. Shishkin, S. Inagaki, K.Y Watanabe,
Possible Control Scenario of Radial Electric Field by Loss-Cone-Particle Injection into Helical Device, Aug 1999

NIFS-608 R Tanaka, T Nakamura and T Yabe,
Constructing Exactly Conservative Scheme in Non-conservative Form, Aug 1999

NIFS-609 H. Sugama,
Gyrokinetic Field Theory, Aug. 1999

NIFS-610 M. Takechi, G. Matsunaga, S. Takagi, K Ohkuni, K. Toi, M Osakabe, M Isobe, S. Okamura, K. Matsuoka, A. Fujisawa, H. Iguchi, S. Lee, T Minami, K. Tanaka, Y. Yoshimura and CHS Group,
Core Localized Toroidal Alfven Eigenmodes Destabilized By Energetic Ions in the CHS Heliotron/Torsatron; Sep. 1999

NIFS-611 K. Ichiguchi,
MHD Equilibrium and Stability in Heliotron Plasmas, Sep 1999

NIFS-612 Y Sato, M. Yokoyama, M. Wakatani and V D Pusovitov
Complete Suppression of Pfirsch-Schluter Current in a Toroidal l=3 Stellarator, Oct. 1999

NIFS-613 S. Wang, H. Sanuki and H. Sugama,
Reduced Drift Kinetic Equation for Neoclassical Transport of Helical Plasmas in Ultra-low Collisionality Regime; Oct. 1999

NIFS-614 J. Miyazawa, H Yamada, K. Yasui, S. Kato, N , Fukumoto, M. Nagata and T. Uyama,
Design of Spheromak Injector Using Conical Accelerator for Large Helical Device, Nov 1999

NIFS-615 M. Uchida, A. Fukuyama, K. Itoh, S.-I. Itoh and M Yagi,
Analysis of Current Diffusive Ballooning Mode in Tokamaks; Dec. 1999

NIFS-616 M. Tanaka, A.Yu Grosberg and T. Tanaka ,
Condensation and Swelling Behavior of Randomly Charged Multichain Polymers by Molecular Dynamics Simulations; Dec. 1999

NIFS-617 S. Goto and S. Kida,
Sparseness of Nonlinear Coupling, Dec 1999

NIFS-618 M.M. Skoric, T Sato, A. Maluckov and M.S Jovanovic,
Complexity in Laser Plasma Instabilities Dec. 1999

NIFS-619 T.-H. Watanabe, H. Sugama and T Sato,
Non-dissipative Kinetic Simulation and Analytical Solution of Three-mode Equations of Ion Temperature Gradient Instability, Dec 1999

NIFS-620 Y Oka, Y Takeiri, Yu.I.Belchenko. M. Hamabe, O. Kaneko, K. Tsumori, M. Osakabe, E. Asano, T. Kawamoto, R. Akiyama ,
Optimization of Cs Deposition in the 1/3 Scale Hydrogen Negative Ion Source for LHD-NBI System ;Dec 1999

NIFS-621 Yu.I Belchenko, Y. Oka, O. Kaneko, Y. Takeiri, A. Krivenko, M. Osakabe, K Tsumori, E Asano, T Kawamoto, R. Akiyama,
Recovery of Cesium in the Hydrogen Negative Ion Sources; Dec 1999

NIFS-622 Y. Oka, O. Kaneko, K. Tsumori, Y Takeiri, M. Osakabe, T. Kawamoto, E. Asano, and R Akiyama,
H- Ion Source Using a Localized Virtual Magnetic Filter in the Plasma Electrode: Type I LV Magnetic Filter: Dec 1999

NIFS-623 M. Tanaka, S Kida, S. Yanase and G. Kawahara,

Zero-absolute-vorticity State in a Rotating Turbulent Shear Flow; Jan. 2000

NIFS-624 F. Leuterer, S. Kubo,
Electron Cyclotron Current Drive at $\omega \approx \omega_c$ with X-mode Launched from the Low Field Side; Feb. 2000

NIFS-625 K. Nishimura,
Wakefield of a Charged Particulate Influenced by Emission Process of Secondary Electrons; Mar. 2000

NIFS-626 K. Itoh, M. Yagi, S.-I. Itoh, A. Fukuyama,
On Turbulent Transport in Burning Plasmas; Mar 2000

NIFS-627 K. Itoh, S.-I. Itoh, L. Giannone,
Modelling of Density Limit Phenomena in Toroidal Helical Plasmas; Mar. 2000

NIFS-628 K. Akaishi, M. Nakasuga and Y. Funato,
True and Measured Outgassing Rates of a Vacuum Chamber with a Reversibly Absorbed Phase; Mar. 2000

NIFS-629 T. Yamagishi,
Effect of Weak Dissipation on a Drift Orbit Mapping, Mar. 2000

NIFS-630 S. Toda, S.-I. Itoh, M. Yagi, A. Fukuyama and K. Itoh,
Spatial Structure of Compound Dither in L/H Transition; Mar. 2000

NIFS-631 N. Ishihara and S. Kida,
Axial and Equatorial Magnetic Dipoles Generated in a Rotating Spherical Shell; Mar. 2000

NIFS-632 T. Kuroda, H. Sugama, R. Kanno and M. Okamoto,
Ion Temperature Gradient Modes in Toroidal Helical Systems; Apr 2000

NIFS-633 V.D. Pustovitov,
Magnetic Diagnostics: General Principles and the Problem of Reconstruction of Plasma Current and Pressure Profiles in Toroidal Systems; Apr. 2000

NIFS-634 A.B. Mikhailovskii, S.V. Konovalov, V.D. Pustovitov and V.S. Tsypin,
Mechanism of Viscosity Effect on Magnetic Island Rotation; Apr 2000

NIFS-635 H. Naitou, T. Kuramoto, T. Kobayashi, M. Yagi, S. Tokuda and T. Matsumoto,
Stabilization of Kinetic Internal Kink Mode by Ion Diamagnetic Effects; Apr. 2000

NIFS-636 A. Kageyama and S. Kida,
A Spectral Method in Spherical Coordinates with Coordinate Singularity at the Origin; Apr. 2000

NIFS-637 R. Horiuchi, W. Pei and T. Sato,
Collisionless Driven Reconnection in an Open System; June 2000

NIFS-638 K. Nagaoka, A. Okamoto, S. Yoshimura and M.Y. Tanaka,
Plasma Flow Measurement Using Directional Langmuir Probe under Weakly Ion-Magnetized Conditions; July 2000

NIFS-639 Alexei Ivanov,
Scaling of the Distribution Function and the Critical Exponents near the Point of a Marginal Stability under the Vlasov-Poisson Equations; Aug. 2000